Society of Medical Education & Research

2024, Volume 4, Issue 2, Page No: 18-28
ISSN: 3108-4834

Archive of International Journal of Cancer and Allied Science

Interaction of Twenty-Seven Bicyclo Derivatives with VEGF Receptors as a Cancer Treatment Alternative

Maria Lopez-Ramos[1], Lauro FigueroaValverde[1*], Marcela Rosas-Nexticapa[2], Magdalena AlvarezRamirez[2], Virginia Mateu-Armand[2], Regina CauichCarrillo[3]

[1]Pharmacochemistry Research Laboratory, Faculty of BiologicalChemical Sciences, University Autonomous of Campeche, Humberto Lanz Cárdenas s/n, Ex Hacienda Kalá, C.P. 24085, Campeche, Mexico.
[2]Nutrition Laboratory, Faculty of Nutrition, University of Veracruz, Medicos y s/n Odontologos 910210, Unidad del Bosque, Xalapa, Mexico.
[3]University Autonomous of Quintana Roo State, Campus Chetumal, Av Erik Paolo Martinez s/nesq. Av. 4 de marzo, Col. Magisterial, C.P. 77039, México.

***E-mail** ✉ lfiguero@uacam.mx

Abstract

Angiogenesis is a key factor in cancer progression, which is influenced by the expression of VEGFR-1, VEGFR-2, and VEGFR-3. Several therapeutic agents, including axitinib, regorafenib, cediranib, and sorafenib, are commonly used in treating cancer, although they can cause side effects such as thrombocytopenia and leukopenia. The current study sought to evaluate how bicyclo derivatives (1-27) interact with VEGFR-1, VEGFR-2, and VEGFR-3, using the 3hng, 2oh4, and 4sbj proteins, along with axitinib, cediranib, regorafenib, and sorafenib as controls in the DockingServer software. The results showed that the bicyclo derivatives bind to specific areas of the 3hng, 2oh4, and 4sbj proteins when compared to the reference drugs. In addition, the inhibition constants (Ki) for bicyclo compounds 1 and 5 were lower than those of axitinib, cabozatinib, cediranib, pazopanib, and regorafenib in their interaction with the 3hng protein. For the 2oh4 protein, derivatives 4, 7, 8, 10, 12, and 15-22 showed lower Ki values than cabozatinib and cediranib. Finally, the interaction of bicyclo analogs 4, 6-8, 10, 12, 13, 16, 18-21, 23, 24, and 26 with the proteins yielded lower Ki values compared to axitinib and cediranib. These findings suggest that specific bicyclo derivatives could be potential anticancer agents by regulating the expression of VEGFR-1, VEGFR-2, and VEGFR-3.

Keywords: VEGFR-1, Cancer, Axitinib, Byciclo, Cediranib

Introduction

Cancer is widely recognized as a significant public health issue globally, with a profound impact on the quality of life of affected populations [1-4]. Various factors have been identified as contributors to cancer development, including hormone imbalances [5, 6], smoking [7], lifestyle choices [8], alcohol consumption [9], and diet [10]. Furthermore, there is evidence suggesting that angiogenesis plays a critical role in the development of several types of cancer [11-13], and is regulated by key biomolecules, such as vascular endothelial growth factor (VEGF), which is essential for tumor progression [14]. VEGF expression can be induced by factors like hypoxia [15], pH alterations [16], and the activation of interleukin-6 [17]. This process may lead to interactions with specific receptors found on the surface of endothelial cells, including VEGFR-1, VEGFR-2, and VEGFR-3, which are frequently expressed in various cancers [18-20]. For instance, research has shown that VEGF can trigger the formation of new lymphatic vessels in gastric cancer patients through the activation of VEGFR-3 [21].

Access this article online https://smerpub.com/

Received: 04 June 2024; **Accepted:** 04 September 2024

Copyright CC BY-NC-SA 4.0

How to cite this article: Lopez-Ramos M, FigueroaValverde L, Rosas-Nexticapa M, AlvarezRamirez M, Mateu-Armand V, CauichCarrillo R. Interaction of Twenty-Seven Bicyclo Derivatives with VEGF Receptors as a Cancer Treatment Alternative. Arch Int J Cancer Allied Sci. 2024;4(2):18-28. https://doi.org/10.51847/m9NoOahmoL

Research indicates a positive correlation between the expression of VEGFR-3 and metastatic lymph node presence in cancer patients [22]. Further findings show that ovarian cancer patients exhibit VEGFR-2 and VEGFR-3 expression, identified through the Western blotting technique [23]. Additionally, Western immunoblotting has revealed the expression of both VEGFR-1 and VEGFR-2 in bladder squamous cell carcinoma cell lines [24]. Nagano *et al.* [25] also highlighted that VEGFR-1 influences epidermal growth factor receptor activity, contributing to the growth of colon cancer cells, as shown by Western blot results.

In terms of pharmacological interventions, various VEGFR-1, VEGFR-2, and VEGFR-3 inhibitors have been explored for their anticancer potential. One study demonstrated that axitinib could reduce metastatic renal cell carcinoma by targeting these VEGF receptors [26]. In another investigation, axitinib exhibited significant anticancer activity in epithelial ovarian cancer by inhibiting VEGF receptor signaling, leading to changes in cell proliferation, apoptosis, and migration [27]. Similarly, regorafenib, a non-selective VEGF receptor antagonist, has been shown to improve survival rates in patients with metastatic colorectal cancer [28]. Combining regorafenib with avelumab also displayed promising antitumor activity in biliary tract cancer patients [29], though some studies suggest regorafenib may promote resistance in colorectal cancer cells through VEGF receptor inhibition [30]. In addition, sorafenib, which targets VEGFR-1, VEGFR-2, and VEGFR-3, has been associated with improved survival in individuals with advanced hepatocellular carcinoma [31]. Other studies point to its potential as a VEGFR-1 inhibitor in AG1-G1-Flt-1 cell lines [32]. These findings suggest that numerous cancer therapies exert their effects through the inhibition of VEGFR receptors. However, the exact mechanisms of these interactions remain unclear, likely due to differences in experimental methods. The current study aims to investigate how twenty-seven bicyclo derivatives interact with VEGFR-1, VEGFR-2, and VEGFR-3 using a theoretical model.

Materials and Methods

The structures of twenty-seven bicyclic derivatives are presented in **Figure 1**, where their interactions with the VEGFR-1, VEGFR-2, and VEGFR-3 cell surface receptors were investigated.

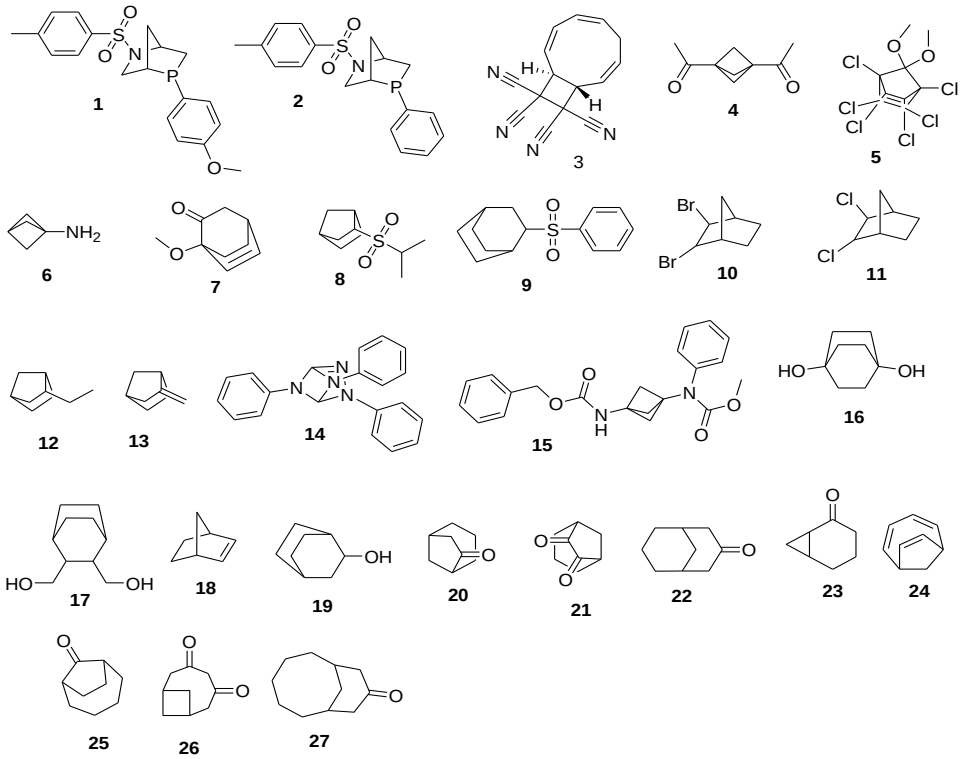

Figure 1. Chemical structure of bicyclo derivatives (1-27); 1 = 5-(4-methoxyphenyl)-2-(p-tolylsulfonyl)-2-aza-5-phosphabicyclo[2.2.1]heptane, 2 = 5-phenyl-2-(p-tolylsulfonyl)-2-aza-5-phosphabicyclo[2.2.1]heptane, 3 =

(1S,2Z,4Z,7Z,9S)-bicyclo[7.2.0]undeca-2,4,7-triene-10,10,11,11-tetracarbonitrile, 4 = 1-(3-acetyl-1-bicyclo[1.1.1]pentanyl)ethanone, 5 = 1,2,3,4,5,6-hexachloro-7,7-dimethoxy-bicyclo[2.2.1]hept-2-ene, 6 = bicyclo[1.1.1]pentan-1-amine, 7 = 1-methoxybicyclo[2.2.2]oct-5-en-2-one, 8 = 2-isopropylsulfonylnorbornane, 9 = 2-(benzenesulfonyl)bicyclo[2.2.2]octane, 10 = 2,3-dibromonorbornane, 11 = 2,3-dichloronorbornane, 12 = 2-ethylnorbornane, 13 = 2-methylenenorbornane, 14 = 3,5,6-triphenyl-2,3,5,6-tetrazabicyclo[2.1.1]hex-1-ene, 15 = methyl N-[3-(benzyloxycarbonylamino)-1-bicyclo[1.1.1]pentanyl]-N-phenyl-carbamate, 16 = bicyclo[2.2.2]octane-1,4-diol, 17 = [3-(hydroxymethyl)-2-bicyclo[2.2.2]octanyl]methanol, 18 = bicyclo[2.2.1]hept-2-ene, 19 = bicyclo[2.2.2]octan-2-ol, 20 = bicyclo[3.2.1]octan-6-one, 21 = bicyclo[3.2.1]octane-6,7-dione, 22 = bicyclo[3.3.1]nonan-3-one, 23 = norcaran-2-one, 24 = bicyclo[4.2.1]nona-2,4,7-triene, 25 = bicyclo[4.2.1]nonan-9-one, 26 = bicyclo[5.1.1]nonane-3,5-dione, 27 = bicyclo[5.3.1]undecan-9-one (Source: https://pubchem.ncbi.nlm.nih.gob).

Ligand-protein complex

The interactions between bicyclic derivatives (1–30) and the VEGFR1, VEGFR2, and VEGFR3 receptors were assessed by employing the 2oh4 [33], 3hng [34], and 4bsj [35] protein structures as models. Additionally, axinib, cediranib, cabozatinib, and sorafenib were selected as control compounds in the DockingServer software [34].

Results and Discussion

Several computational tools such as AutoDock, USFDock, rDock, and LeDock [36] have been utilized for studying the binding of various drugs with biomolecular targets. Previous studies have shown that DockingServer is a reliable platform for evaluating anticancer drug interactions. For instance, a theoretical model indicated that boswellic acid may exhibit anticancer activity through its binding to CDK2 (cell division protein kinase 2) when using ArgusLab 4.0.1 software [37]. In a similar context, DockingServer was also used to explore how quinolone derivatives bind to RSK-4 (ribosomal S6 kinase 4), suggesting that these compounds could play a role in inhibiting cancer progression [38]. This study focused on determining how twenty-seven bicyclic derivatives interact with VEGFR-1, VEGFR-2, and VEGFR-3, using 3hng, 2oh4, and 4bsj proteins in the DockingServer tool. For comparative analysis, axinib, cediranib, cabozatinib, pazonib, regorafenib, and sorafenib were employed as reference drugs. The interaction analysis revealed significant differences in the amino acid residues involved in binding the bicyclic derivatives (compounds 1–27) to the 3hng protein surface, as compared to the interactions observed with the control drugs like axinib, cabozatinib, pazonib, cediranib, and regorafenib **(Table 1)**.

Table 1. Interaction of bicyclic derivatives (1-27), axitinib, cabozantinib, pazopanib, and regorafenib with amino acid residues of 3hng protein surface

Compound	Aminoacid residues
Axitinib	Val_{841}; Glu_{878}; Ile_{881}; Leu_{882}; Val_{891}; Val_{892}; Leu_{1013}; Cys_{1018}; His_{1020}; Leu_{1029}; Ile_{1038}; Cys_{1039}; Asp_{1040}; Phe_{104}
Cabozantinib	Val_{841}; Ala_{859}; Lys_{861}; $Glu8_{78}$; Ile_{881}; Leu_{882}; Val_{892}; Val_{907}; Val_{909}; Cys_{1018}; His_{1020}; Leu_{1029}; Ile_{1038}; Cys_{1039}; Asp_{1040}; Phe_{1041}
Pazopanib	Leu_{833}; Glu_{878}; Leu_{882}; Val_{892}; Val_{909}; Tyr_{911}; Cys_{912}; His_{1020}; Leu_{1029}; Cys_{1039}; Asp_{1040}; Phe_{1041}
Regorafenib	Val_{841}; Ala_{859}; Lys_{861}; Glu_{878}; Leu_{882}; Ile_{885}; Ile_{881}; Val_{892}; Val_{907}; Val_{909}; Cys_{912}; Leu_{1013}; Cys_{1018}; Ile_{1019}; His_{1020}; Leu_{1029}; Asp_{1040}; Phe_{1041}
1	Val_{841}; Lys_{861}; Glu_{878}; Ile_{881}; Leu_{882}; Ile_{885}; Val_{892}; Leu_{1013}; Cys_{1018}; His_{1020}; Ile_{1038}; Cys_{1039}; Asp_{1040}; Phe_{1041}
2	Val_{841}; Ala_{859}; Lys_{861}; Glu_{878}; Leu_{882}; Val_{891}; Val_{892}; Val_{909}; Cys_{912}; Leu_{1029}; Cys_{1039}; Phe_{1041}
3	Glu_{878}; Ile_{881}; Leu_{882}; Ile_{885}; Val_{891}; Leu_{1013}; Cys_{1018}; His_{1020}; Ile_{1038}; Asp_{1040}
4	Val_{841}; Lys_{861}; Glu_{878}; Leu_{882}; Val_{892}; Val_{909}; Asp_{1040}
5	Asp_{807}; Thr_{877}; Glu_{878}; Ile_{881}; Ile_{1019}; Arg_{1021}; Asp_{1040}
6	Cys_{1018}; His_{1020}; Asp_{1040}
7	Val_{841}; Ala_{859}; Lys_{861}; Glu_{878}; Val_{892}; Val_{909}; Leu_{1029}; Cys_{1039}; Phe_{1041}

8	Val_{841}; Ala_{859}; Lys_{861}; Glu_{878}; Val_{892}; Val_{909}; Leu_{1029}; Cys_{1039}
9	Glu_{878}; Ile_{881}; Leu_{882}; Ile_{885}; Val_{891}; Leu_{1013}; Cys_{1018}; His_{1020}; Ile_{1038}; Asp_{1040}
10	Val_{841}; Ala_{859}; Lys_{861}; Val_{909}; Leu_{1029}; Cys_{1039}; Phe_{1041}
11	Val_{841}; Lys_{861}; Glu_{878}; Val_{909}; Leu_{1029}; Cys_{1039}; Asp_{1040}; Phe_{1041}
12	Val_{841}; Ala_{859}; Lys_{861}; Val_{909}; Cys_{1039}
13	Val_{841}; Lys_{861}; Val_{909}; Cys_{1039}; Phe_{1041}
14	Asp_{807}; Glu_{878}; Ile_{881}; Leu_{1013}; Cys_{1018}; His_{1020}; Arg_{1021}; Ile_{1038}; Asp_{1040}
15	Ala_{859}; Lys_{861}; Glu_{878}; Ile_{881}; Leu_{882}; Ile_{885}; Val_{891}; Val_{892}; Val_{909}; Leu_{1013}; Cys_{1018}; Leu_{1029}; Cys_{1039}; Asp_{1040}
16	Val_{841}; Ala_{859}; Lys_{861}; Val_{892}; Val_{909}; Leu_{1029}; Cys_{1039}; Phe_{1041}
17	Val_{841}; Lys_{861}; Glu_{878}; Leu_{882}; Val_{892}; Val_{907}; Val_{909}; Leu_{1029}; Cys_{1039}; Phe_{1041}
18	Val_{841}; Lys_{861}; Val_{909}; Leu_{1029}; Cys_{1039}; Phe_{1041}
19	Val_{841}; Lys_{861}; Glu_{878}; Val_{892}; Val_{909}; Cys_{1039}; Phe_{1041}
20	Val_{841}; Ala_{859}; Lys_{861}; Val_{892}; Val_{909}; Cys_{1039}
21	Val_{841}; Ala_{859}; Lys_{861}; Val_{892}; Val_{909}; Cys_{1039}
22	Val_{841}; Ala_{859}; Lys_{861}; Val_{892}; Val_{909}; Leu_{1029}; Cys_{1039}; Phe_{1041}
23	Val_{841}; Lys_{861}; Glu_{878}; Val_{909}
24	Val_{841}; Ala_{859}; Lys_{861}; Glu_{878}; Val_{892}; Val_{909}
25	Val_{841}; Ala_{859}; Lys_{861}; Glu_{878}; Val_{892}; Val_{909}; Cys_{1039}; Phe_{1041}
26	Val_{841}; Ala_{859}; Lys_{861}; Val_{909}; Leu_{1029}; Cys_{1039}; Phe_{1041}
27	Val_{841}; Ala_{859}; Lys_{861}; Glu_{878}; Leu_{882}; Val_{892}; Val_{909}; Cys_{1039};

Other findings reveal that the inhibition constant (Ki) for compounds 1 and 15 was significantly lower than that of axinib, cabozatinib, cediranib, pazonib, and regorafenib **(Table 2)**. Specifically, compound 1 appears to interact with the 3hng protein surface via a hydrophobic bond with Leu882 and a polar interaction with His102. On the other hand, compound 15 seems to bind through hydrogen bonds with Glu878 and Asp1040 on the 3hng protein surface.

Table 2. Various energies at which carbazole analogs (1-26), decernotinib, and facitinib bind to the 3pjc protein surface

Compound	A	B	C	D	E	F
Axitinib	-9.60	91.30	-10.00	-0.07	-10.07	886.38
Cabozantinib	-7.70	2.28	-8.77	-0.18	-8.95	1000.65
Pazopanib	-8.76	380.77	-10.15	-0.11	-10.26	999.38
Regorafenib	-5.05	198.17	-6.84	-0.09	-6.93	1004.77
1	-8.18	1.01	-9.13	-0.09	-9.22	832.63
2	-8.86	322.19	-9.76	-0.05	-9.81	778.327
3	-5.43	103.85	-6.76	+0.13	-6.62	601.43
4	-5.29	132.14	-5.78	-0.11	-5.89	452.762
5	-5.29	131.89	-5.91	-0.09	-6.00	618.227
6	-4.41	588.45	-3.42	-1.29	-4.71	324.656
7	-5.39	111.96	-5.65	-0.04	-5.69	442.002
8	-6.25	26.34	-6.72	-0.07	-6.79	506.598
9	-6.66	13.13	-7.14	+0.05	-7.09	577.614
10	-5.45	101.04	-5.46	+0.00	-5.45	328.935
11	-6.51	16.89	-6.54	+0.03	-6.51	420.898

12	-5.27	138.19	-5.56	-0.00	-5.56	378.072
13	-4.73	339.02	4.73	-0.00	-4.73	353.959
14	-6.93	8.30	-7.66	-0.01	-7.67	757.683
15	-7.82	1.85	-9.93	-0.05	-9.98	896.067
16	-4.63	404.38	-5.14	-0.09	-5.23	405.007
17	-6.74	11.50	-6.81	-0.09	-6.90	57.287
18	-4.13	932.21	-4.14	+0.00	-4.13	328.053
19	-4.96	233.30	-5.21	-0.05	-5.25	369.284
20	-5.02	210.70	-5.03	+0.01	-5.02	361.576
21	-5.27	137.86	-5.34	+0.07	-5.27	397.849
22	-5.53	88.52	-5.55	+0.02	-5.53	411.912
23	-4.46	540.62	-4.45	-0.01	-4.46	330.74
24	-5.33	123.09	-5.35	+0.01	-5.33	354.272
25	-5.52	90.67	-5.45	-0.06	-5.52	406.755
26	-5.77	58.74	-5.76	-0.02	-5.77	423.77
27	-6.85	9.52	-6.85	+0.00	-6.85	459.872

A = Est: free energy of binding (kcal/mol); B = Est. inhibition constant, Ki (mM); C = vdW + Hbond + desolv energy (kcal/mol); D = electrostatic energy (kcal/mol); E = total intermolec energy (kcal/mol); and F = interact surface

Other findings reveal that the binding of bicyclic derivatives (compounds 1-27) to the 2oh4 protein resulted in distinct differences in the amino acid residues on the protein surface, especially when contrasted with the binding patterns of cabozantinib and cediranib **(Table 3)**.

Table 3. Coupling of bicyclic derivatives (1-27), cabozantinib, and cediranib with amino acid residues of 2oh4 protein surface

Compound	Aminoacid residues
Cabozantinib	Arg_{840}; Arg_{1049}; Ile_{1051}; Lys_{1053}; Asp_{1054}
Cediranib	Arg_{840}; Lys_{869}; Arg_{1049}; Lys_{1053}; Asp_{1054}; Pro_{1055}
1	Arg_{840}; Lys_{869}; Lys_{1053}; Asp_{1054}; Pro_{1055}
2	Arg_{840}; Ala_{842}; Lys_{869}; Arg_{1049}; Lys_{1053}; Asp_{1054}
3	Arg_{840}; Gly_{841}; Ala_{842}; Lys_{869}; Asp_{1054}
4	Arg_{1030}; Arg_{1049}; Asp_{1050}; Ala_{1063}; Pro_{1066}
5	Pro_{837}; Arg_{840}; Arg_{1049}; Lys_{1053}
6	Asp_{1054}; Pro_{1055}; Asp_{1056}
7	Arg_{1030}; Ala_{1048}; Asp_{1050}; Ile_{1051}; Arg_{1064}; Pro_{1066}
8	Arg_{840}; Lys_{1053}
9	Arg_{840}; Lys_{869}; Arg_{1049}; Lys_{1053}; Asp_{1054}
10	Arg_{1030}; Ala_{1048}; Asp_{1050}; Ile_{1051}; Arg_{1064}; Pro_{1066}
11	Arg_{1030}; Ala_{1048}; Asp_{1050}; Ile_{1051}; Arg_{1064}; Pro_{1066}
12	Phe_{843}; Lys_{866}; Leu_{868}; Ala_{879}; Leu_{880}; Glu_{883}
13	Phe_{843}; Lys_{866}; Leu_{868}; Glu_{876}; Ala_{879}; Leu_{880}
14	Pro_{837}; Arg_{840}; Arg_{1030}; Arg_{1049}; Asp_{1050}; Lys_{1053}; Asp_{1062}
15	Arg_{840}; Ala_{842}; Lys_{869}; Arg_{1049}; Lys_{1053}
16	Lys_{869}; Thr_{873}; Glu_{876}
17	Ala_{842}; Lys_{869}

18	Phe_{843}; Lys_{866}; Leu_{868}; Ala_{879}; Leu_{880}
19	Arg_{1030}; Ala_{1048}; Asp_{1050}; Ile_{1051}; Arg_{1064}; Pro_{1066}
20	Arg_{1030}; Asp_{1050}; Ile_{1051}; Pro_{1066}
21	Arg_{1030}; Ala_{1048}; Asp_{1050}; Ile_{1051}; Arg_{1064}; Pro_{1066}
22	Arg_{840}; Lys_{869}
23	Phe_{843}; Lys_{866}; Leu_{868}; Glu_{876}; Ala_{879}; Leu_{880}
24	Phe_{843}; Lys_{866}; Leu_{868}; Glu_{876}; Ala_{879}; Leu_{880}; Glu_{883}
25	Arg_{1030}; Asp_{1050}; Arg_{1064}; Pro_{1066}
26	Asp_{1026}; Arg_{1030}; Asp_{1050}; Ile_{1051}; Arg_{1064}; Pro_{1066}
27	Arg_{1030}; Ala_{1048}; Asp_{1050}; Ile_{1051}; Pro_{1066}

The inhibition constants (Ki) for bicyclic derivatives 4, 7, 8, 10, 12, and 15-22 were found to be lower than those for cabozantinib and cediranib **(Table 4)**. This observation could be linked to the way these compounds engage with specific amino acid residues. For instance, compound 4 might interact via a hydrogen bond with Arg1049 and a hydrophobic bond with Pro1066, while compound 7 could form hydrophobic bonds with Ala1048, Ile1051, and Pro1066. Compound 8 might bind to Arg840 and Lys1053, and compound 10 may form a hydrogen bond with Arg1064 alongside hydrophobic interactions with Ala1048 and Ile1051. For compound 12, hydrophobic interactions could occur with Phe843, Leu868, Ala879, and Leu880. Compound 15 might engage through a hydrogen bond with Arg840 and hydrophobic bonds with Ala842. In the case of compound 16, a polar interaction with Glu876 is likely, while compound 17 may interact with Ala842 and Lys869. Compound 18 could form hydrophobic bonds with Phe843, Leu868, Ala879, and Leu880, while compound 19 might form polar interactions with Arg1030 and Arg1064, as well as hydrophobic bonds with Ala1048, Ile1051, and Pro1060. Compound 20 could bind through a polar bond with Arg1030 and hydrophobic interactions with Ile1051 and Pro1066, while compound 21 might interact through polar bonds with both Arg1030 and Arg1064, as well as hydrophobic bonds with Ala1048, Ile1051, and Pro1066. Lastly, compound 22 may engage with Arg840 and Lys869.

Table 4. Thermodynamics parameters involved in the interaction of bicyclic derivatives (1-27), cabozantinib, and cediranib with 2oh4 protein surface

Compound	A	B	C	D	E	F
Cabozantinib	-5.15	168.22	-5.81	-0.18	-5.99	671.90
Cediranib	-4.53	474.23	-4.75	-0.39	-5.14	615.74
1	-4.32	686.33	-5.31	-0.14	-5.44	593.403
2	-4.66	380.73	-5.55	+0.00	-5.55	625.531
3	-4.21	825.61	-5.30	-0.10	-5.40	509.798
4	-3.72	1.88	-4.15	-0.17	-4.32	486.822
5	-4.83	289.72	-5.21	-0.01	-5.23	512.918
6	-4.32	684.73	-2.17	-2.44	-4.62	185.871
7	-3.69	1.96	-3.78	-0.21	-3.99	437.277
8	-3.68	1.99	-4.22	-0.06	-4.27	453.462
9	-4.62	412.93	-5.29	+0.07	-5.22	517.217
10	-4.00	1.17	-3.95	-0.05	-4.00	307.113
11	-4.50	501.37	-4.44	-0.06	-4.50	392.868
12	-3.85	1.52	-4.14	-0.00	-4.14	346.732
13	-4.13	939.89	-4.13	-0.00	-4.13	311.138
14	-6.64	13.48	-7.31	-0.05	-7.36	662.596

15	-3.94	1.29	-6.15	+0.06	-6.08	678.07
16	-3.37	3.37	-3.64	-0.33	-3.97	309.652
17	-3.80	1.64	-3.67	-0.06	-3.73	398.224
18	-3.65	2.10	-3.65	-0.00	-3.65	285.446
19	-3.65	2.11	-3.84	-0.11	-3.95	338.907
20	-3.90	1.39	-3.79	-0.11	-3.90	334.548
21	-4.05	1.08	-3.87	-0.17	-4.05	370.26
22	-3.56	2.44	-3.70	+0.13	-3.56	351.532
23	-4.16	887.31	-4.13	-0.03	-4.16	307.633
24	-4.31	696.25	-4.32	+0.01	-4.31	322.443
25	-4.15	910.75	-3.98	-0.17	-4.15	388.441
26	-3.96	1.26	-4.04	+0.09	-3.96	413.098
27	-4.43	570.49	-4.31	-0.11	-4.43	443.151

A = Est: free energy of binding (kcal/mol); B = Est. inhibition constant, Ki (mM); C = vdW + Hbond + desolv energy (kcal/mol); D = electrostatic energy (kcal/mol); E = total intermolec energy (kcal/mol); and F = interact surface

In conclusion, other findings **(Table 5)** show discrepancies in the number of amino acid residues involved in the binding of bicyclic derivatives 1-27 to the 4sbj protein surface when compared to axitinib and cediranib.

Table 5. Coupling of bicyclic derivatives (1-27), axitinib, and cediranib with amino acid residues of 4sbj protein surface

Compound	**Aminoacid residues**
Axitinib	Ala_{400}; Leu_{401}; Trp_{402}; Arg_{409}; Arg_{410}; Asn_{411}
Cediranib	Tyr_{369}; Ala_{400}; Trp_{402}; Arg_{409}; Asn_{411}
1	Tyr_{369}; Thr_{398}; Ala_{400}; Trp_{402}; Ser_{404}; Arg_{409}; Asn_{411}
2	Tyr_{369}; Thr_{398}; Ala_{400};, Arg_{409}; Asn_{411}
3	Tyr_{369}; Ala_{400}; Trp_{402}; Arg_{409}; Asn_{411}
4	Ala_{400}; Trp_{402}; Arg_{409}; Asn_{411}
5	Tyr_{369}; Ala_{400}; Leu_{401}; Trp_{402}; Arg_{409}; Asn_{411}
6	Ala_{400}; Leu_{401}; Trp_{402}; Arg_{409}; Arg_{410}; Asn_{411}
7	Ala_{400}; Trp_{402}; Arg_{409}; Asn_{411}
8	Ala_{400}; Trp_{402}; Arg_{409}; Asn_{411}
9	Tyr_{369}; Ala_{400}; Trp_{402}; Arg_{409}; Asn_{411}
10	Tyr_{369}; Ala_{400}; Trp_{402}; Arg_{409}; Asn_{411}
11	Tyr_{369}; Ala_{400}; Trp_{402}; Arg_{409}; Asn_{411}
12	Ala_{400}; Trp_{402}; Arg_{409}; Asn_{411}
13	Ala_{400}; Trp_{402}; Arg_{409}; Asn_{411}
14	Tyr_{369}; Thr_{398}; Ala_{400}; Trp_{402}; Asn_{411}
15	Tyr_{369}; Thr_{398}; Ala_{400}; Trp_{402}; Arg_{409}; Asn_{411}
16	Ala_{400}; Trp_{402}; Arg_{409}; Asn_{411}
17	Tyr_{369}; Ala_{400}; Trp_{402}; Arg_{409}; Asn_{411}
18	Ala_{400}; Trp_{402}; Arg_{409}; Asn_{411}
19	Ala_{400}; Trp_{402}; Arg_{409}; Asn_{411}
20	Ala_{400}; Trp_{402}; Arg_{409}; Asn_{411}
21	Ala_{400}; Trp_{402}; Arg_{409}; Asn_{411}

22	Ala_{400}; Trp_{402}; Arg_{409}; Asn_{411}
23	Ala_{400}; Trp_{402}; Arg_{409}; Asn_{411}
24	Ala_{400}; Trp_{402}; Arg_{409}; Asn_{411}
25	Ala_{400}; Trp_{402}; Arg_{409}; Asn_{411}
26	Ala_{400}; Trp_{402}; Arg_{409}; Asn_{411}
27	Trp_{402}; Arg_{409}; Asn_{411}

The inhibition constants (Ki) for bicyclic derivatives 4, 6-8, 10, 12, 13, 16, 18-21, 23, 24, and 26 were found to be more favorable compared to axitinib and cediranib. This variation can be attributed to how each derivative interacts with specific amino acid residues on the protein surface. For instance, compound 4 **(Table 6)** appears to form a polar interaction with Arg4090 and Asn411, alongside hydrophobic interactions involving Ala400 and Trp402. Compound 6 binds through hydrogen bonding with Leu401, Arg410, and Asn411, as well as hydrophobic interactions with Ala400 and Trp402. The binding pattern of compound 7 involves polar interaction with Arg409 and hydrophobic bonding with Ala400 and Trp402. Compound 8 primarily shows hydrophobic binding with Ala400 and Trp402. In compound 10, the interaction is largely hydrophobic, with additional halogen bonding with Tyr369. Both compounds 12 and 13 exhibit hydrophobic bonding with Ala400 and Trp402. Compound 16's interactions include polar bonding with Arg409 and Asn411, combined with hydrophobic interactions involving Ala400 and Trp402. Compound 18 also forms hydrophobic bonds with Ala400 and Trp402, while compound 19 shows polar interaction with Asn411 and hydrophobic binding with Ala400 and Trp402. Compound 20 predominantly engages in hydrophobic bonding with Ala400 and Trp402. For compound 21, both polar interaction with Arg409 and hydrophobic binding with Ala400 and Trp402 are observed. Compound 23 shows hydrophobic interaction with Ala400, as well as a pi-pi bond with Trp402. Both compounds 24 and 26 demonstrate hydrophobic binding with Ala400 and Trp402.

Table 6. Thermodynamics parameters involved in the interaction of bicyclic derivatives (1-27), axitinib, and cediranib with 4bsj protein surface

Compound	A	B	C	D	E	F
Axitinib	-6.96	7.87	-7.74	0.00	-7.74	629.46
Cediranib	-4.92	248.37	-4.71	0.11	-4.60	475.52
1	-4.83	288.81	-6.05	+0.02	-6.03	642.309
2	-4.75	327.53	-5.53	-0.01	-5.54	571.586
3	-4.26	756.37	-5.41	-0.04	-5.45	468.482
4	-3.27	4.04	-3.77	-0.09	-3.86	364.033
5	-4.70	358.24	-5.47	-0.00	-5.47	461.545
6	-3.32	3.71	-3.52	-0.10	-3.61	265.362
7	-3.93	1.32	-4.04	-0.18	-4.22	361.663
8	-3.87	1.47	-4.43	+0.03	-4.41	407.43
9	-4.65	392.57	-4.94	-0.07	-5.02	429.595
10	-3.97	1.24	-3.95	-0.02	-3.97	266.541
11	-4.48	520.45	-4.46	-0.01	-4.48	345.514
12	-3.92	1.35	-4.21	-0.00	-4.21	311.676
13	-3.87	1.46	-3.87	-0.00	-3.87	289.115
14	-4.44	555.92	-5.15	-0.00	-5.15	545.316
15	-4.21	826.34	-6.10	+0.02	-6.08	659.82
16	-3.23	4.30	-3.79	-0.04	-3.83	324.767
17	-4.73	343.36	-4.66	-0.02	-4.68	381.591

18	-3.56	2.44	-3.56	-0.01	-3.56	263.194
19	-3.84	1.53	-4.11	-0.03	-4.14	299.916
20	-3.99	1.18	-4.00	+0.00	-3.99	289.691
21	-4.02	1.14	-3.95	-0.07	-4.02	328.993
22	-4.25	766.59	-4.17	-0.08	-4.25	345.759
23	-3.50	2.71	-3.51	+0.01	-3.50	278.369
24	-4.05	1.08	-4.04	-0.01	-4.05	292.545
25	-4.18	863.98	-4.11	-0.07	-4.18	338.722
26	-4.04	1.10	-3.97	-0.07	-4.04	333.875
27	-4.45	545.67	-4.43	-0.02	-4.45	365.436

A = Est: free energy of binding (kcal/mol); B = Est. inhibition constant, Ki (mM); C = vdW + Hbond + desolv energy (kcal/mol); D = electrostatic energy (kcal/mol); E = total intermolec energy (kcal/mol); and F = interact surface

Conclusion

The current investigation focused on examining the interaction of bicyclic analogs with VEGFR-1, VEGFR-2, and VEGFR-3 using 3hng, 2oh4, and 4bsj proteins in theoretical models. The key observations from the study were: i) Bicyclic derivatives 1 and 15 exhibited greater binding affinity towards the 3hng protein surface compared to axinib, cabozatinib, cediranib, pazonib, and regorafenib; ii) The inhibition constants (Ki) for the association of compounds 4, 7, 8, 10, 12, and 15-22 with the 2oh4 protein surface were lower than those seen with cabozatinib and cediranib. In addition, the interactions of derivatives 4, 6-8, 10, 12, 13, 16, 18-21, 23, 24, and 26 showed improved values compared to axitinib and cediranib. These results suggest that bicyclic derivatives, particularly 1, 4, 6-8, 10, 12, 13, 15-24, and 26, may have a potential impact on the biological functions of VEGFR-1, VEGFR-2, and VEGFR-3, implying their possible efficacy as anticancer agents.

Acknowledgments: None

Conflict of Interest: None

Financial Support: None

Ethics Statement: None

References

1. Siegel R, Miller K, Wagle N, Jemal A. Cancer statistics, 2023. Cancer J Clin. 2023;73(1):17-48. doi:10.3322/caac.21820
2. Chhikara B, Parang K. Global cancer statistics 2022: The trends projection analysis. Chem Biol Lett. 2022;10(1):451.
3. Shang H, Ning W, Sun J, Guo N, Guo X, Zhang J, et al. Investigation of the quality of life, mental status in patients with gynecological cancer and its influencing factors. World J Psych. 2024;14(7):1053. doi:10.5498%2Fwjp.v14.i7.1053
4. Costa M, Bilobran M, De-Oliveira L, Muniz A, Chelles P, Sampaio S. Correlation between cancer pain and quality of life in patients with advanced cancer admitted to a palliative care unit. Am J Hosp Pall Med. 2024;41(8):882-8. doi:10.1177/10499091231195318
5. Liu Z, Zhang Y, Lagergren J, Li S, Li J, Zhou Z, et al. Circulating sex hormone levels and risk of gastrointestinal cancer: systematic review and meta-analysis of prospective studies. Cancer Epidemiol Biom Prev. 2023;32(7):936-46. doi:10.1158/1055-9965.EPI-23-00396
6. Anbarasu S, Anbarasu A. Cancer-biomarkers associated with sex hormone receptors and recent therapeutic advancements: a comprehensive review. Med Oncol. 2023;40(171):171.
7. Liu Y, Lu L, Yang H, Wu X, Luo X, Shen J, et al. Dysregulation of immunity by cigarette smoking promotes inflammation and cancer: a review. Environ Poll. 2023:122730. doi:10.1016/j.envpol.2023.122730
8. Kwon M, Kang H, Choi H, Kim J, Kim J, Bang W, et al. Risk for esophageal cancer based on lifestyle factors–smoking, alcohol consumption, and body mass index: Insight from a South Korean population study in a low-incidence area. J Clin Med.

2023;12(22):7086. Available from: https://www.mdpi.com/2077-0383/12/22/7086#
9. Shi M, Luo C, Oduyale O, Zong X, LoConte N, Cao Y. Alcohol consumption among adults with a cancer diagnosis in the all of us research program. J Am Med Assoc. 2023;6(8):1-15. Available from: https://jama.jamanetwork.com/article.aspx?doi=10.1001/jamanetworkopen.2023.28328&utm_campaign=articlePDF%26utm_medium=articlePDFlink%26utm_source=articlePDF%26utm_content=jamanetworkopen.2023.28328.
10. Kim S, Park D, Lim Y. Impact of diet on colorectal cancer progression and prevention: from nutrients to neoplasms. Korean J Gastroenterol. 2023;82(2):73-83. Available from: https://orcid.org/0000-0002-3279-332X
11. Lv S, Liu Y, Xie C, Xue C, Du S, Yao J. Emerging role of interactions between tumor angiogenesis and cancer stem cells. J Control Rel. 2023;360:468-81. doi:10.1016/j.jconrel.2023.06.036
12. Melegh Z, Oltean S. Targeting angiogenesis in prostate cancer. Int J Mol Sci. 2019;20(11):1-16. Available from: https://www.mdpi.com/1422-0067/20/11/2676#
13. Ngaha T, Zhilenkova A, Essogmo F, Uchendu I, Abah M, Fossa L, et al. Angiogenesis in lung cancer: understanding the roles of growth factors. Cancers. 2023;15(18):1-16. Available from: https://www.mdpi.com/2072-6694/15/18/4648#
14. Brogowska K, Zajkowska M, Mroczko B. Vascular endothelial growth factor ligands and receptors in breast cancer. J Clin Med. 2023;12(6):2412. doi:10.3390/jcm12062412
15. Namiki A, Brogi E, Kearney M, Kim E, Wu T, Couffinhal T, et al. Hypoxia induces vascular endothelial growth factor in cultured human endothelial cells. J Biol Chem. 1995;270(52):31189-95.
16. Xu L, Fukumura D, Jain R. Acidic extracellular pH induces vascular endothelial growth factor (VEGF) in human glioblastoma cells via ERK1/2 MAPK signaling pathway: mechanism of low pH-induced VEGF. J Biol Chem. 2002;277(13):11368-74.
17. Feurino L, Zhang Y, Bharadwaj U, Zhang R, Li F, Fisher WE, et al. IL-6 stimulates Th2 type cytokine secretion and upregulates VEGF and NRP-1 expression in pancreatic cancer cells. Cancer Biol Ther. 2007;6(7):1096-100. doi:10.4161/cbt.6.7.4328
18. Ahmad A, Nawaz MI. Molecular mechanism of VEGF and its role in pathological angiogenesis. J Cell Biochem. 2022;123(12):1938-65. doi:10.1002/jcb.30344
19. Eguchi R, Kawabe JI, Wakabayashi I. VEGF-independent angiogenic factors: beyond VEGF/VEGFR2 signaling. J Vasc Res. 2022;59(2):78-89. doi:10.1159/000521584
20. Sertoglu E, Yücel Ç, Omma A, Hayran Y, Colak S, Sandıkçı S, et al. Determination of serum vascular endothelial growth factor (VEGF) and VEGF receptor levels with VEGF gene polymorphisms in patients with Behçet's uveitis. Adv Clin Exp Med. 2022;31(3):231-40. doi:10.17219/acem/143586
21. Yonemura Y, Fushida S, Bando E, Kinoshita K, Miwa K, Endo Y, et al. Lymphangiogenesis and the vascular endothelial growth factor receptor (VEGFR)-3 in gastric cancer. Eur J Cancer. 2001;37(7):918-23. doi:10.1016/S0959-8049(01)00015-6
22. Li XF, Zhang XJ, Hao FR, Dong XT, Xu GD, Zhang YX. The pathological roles and potential mechanisms of vascular endothelial growth factor receptor-3 in gastric cancer. J Int Med Res. 2024;52(3):03000605241234558. doi:10.1177/03000605241234558
23. Klasa-Mazurkiewicz D, Jarząb M, Milczek T, Lipińska B, Emerich J. Clinical significance of VEGFR-2 and VEGFR-3 expression in ovarian cancer patients. Polish J Pathol. 2011;62(1):31-40.
24. Kopparapu P, Boorjian S, Robinson B, Downes M, Gudas L, Mongan N. Expression of VEGF and its receptors VEGFR1/VEGFR2 is associated with invasiveness of bladder cancer. Anticancer Res. 2013;33(6):2381-90.
25. Nagano H, Tomida C, Yamagishi N, Teshima-Kondo S. VEGFR-1 regulates EGF-R to promote proliferation in colon cancer cells. Int J Mol Sci. 2019;20(22):1-17. doi:10.3390/ijms20225608
26. Escudier B, Gore M. Axitinib for the management of metastatic renal cell carcinoma. Drugs R & D. 2011;11:113-26.
27. Paik E, Kim T, Cho Y, Ryu J, Choi J, Lee Y, et al. Preclinical assessment of the VEGFR inhibitor axitinib as a therapeutic agent for epithelial ovarian cancer. Sci Rep. 2020;10(1):1-9. doi:10.1038/s41598-020-61871-w
28. Bekaii-Saab T, Ou F, Ahn D, Boland P, Ciombor K, Heying E. Regorafenib dose-optimisation in patients

with refractory metastatic colorectal cancer (ReDOS): a randomised, multicentre, open-label, phase 2 study. Lancet Oncol. 2019;20(8):1070-82.
29. Cousin S, Cantarel C, Guegan J, Mazard T, Gomez-Roca C, Metges J, et al. Regorafenib–avelumab combination in patients with biliary tract cancer (REGOMUNE): a single-arm, open-label, phase II trial. Eur J Cancer. 2022;162:161-9. doi:10.1016/j.ejca.2021.11.012
30. Tomida C, Nagano H, Yamagishi N, Uchida T, Ohno A, Hirasaka K. Regorafenib induces adaptive resistance of colorectal cancer cells via inhibition of vascular endothelial growth factor receptor. J Med Inv. 2017;64(3.4):262-5. doi:10.2152/jmi.64.262
31. Campani C, Rimassa L, Personeni N, Marra F. Angiogenesis inhibitors for advanced hepatocellular carcinoma: In search for the right partner. Ann Trans Med. 2020;8(22):1-7. doi:10.21037%2Fatm-20-3788
32. Brave S, Ratcliffe K, Wilson Z, James N, Ashton S, Wainwright A, et al. Assessing the activity of cediranib, a VEGFR-2/3 tyrosine kinase inhibitor, against VEGFR-1 and members of the structurally related PDGFR family. Mol Cancer Ther. 2011;10(5):861-73. doi:10.1158/1535-7163.MCT-10-0976
33. Hasegawa M, Nishigaki N, Washio Y, Kano K, Harris P, Sato H, et al. Discovery of novel benzimidazoles as potent inhibitors of TIE-2 and VEGFR-2 tyrosine kinase receptors. J Med Chem. 2007;50(18):4453-70. doi:10.1021/jm0611051
34. Figueroa-Valverde L, Díaz-Cedillo F, Rosas-Nexticapa M, Alvarez-Ramirez M, Mateu-Armad M, López-Ramos M, et al. Interaction of some amino-nitrile derivatives with vascular endothelial growth factor receptor 1 (VEGFR1) using a theoretical model. Drug Res. 2023;73(06):355-64. doi:10.1055/a-2062-3571
35. Leppanen V, Torogov D, Kisko K, Prota A, Jeltsch M. Structural and mechanistic insights into VEGF receptor 3 ligand binding and activation. Proc Nat Acad Sci. 2013;110(32):12960-5. doi:10.1073/pnas.1301415110
36. Mahanthesh M, Ranjith D, Yaligar R, Jyothi R, Narappa G, Ravi M. Swiss ADME prediction of phytochemicals present in Butea monosperma (Lam.) Taub J Pharm Phytochem. 2020;9(3):1799-809.
37. Lagunin A, Zakharov A, Filimonov D, Poroikov V. QSAR modelling of rat acute toxicity on the basis of PASS prediction. Mol Inf. 2011;30(23):241-50. doi:10.1002/minf.201000151
38. Bai Q, Liu S, Tian Y, Xu T, BanegasLuna A, PérezSánchez H, et al. Application advances of deep learning methods for de novo drug design and molecular dynamics simulation. Wires: Comp Mol Sci. 2022;12(3):1-19. doi:10.1002/wcms.1581